Cell volume distributions reveal cell growth rates and division times

Michael Halter [a,*], John T. Elliott [a], Joseph B. Hubbard [a], Alessandro Tona [b], Anne L. Plant [a]

[a] Biochemical Science Division, National Institute of Standards and Technology, Gaithersburg, MD 20899, USA
[b] SAIC, Arlington, VA 22201, USA

ABSTRACT

A population of cells in culture displays a range of phenotypic responses even when those cells are derived from a single cell and are exposed to a homogeneous environment. Phenotypic variability can have a number of sources including the variable rates at which individual cells within the population grow and divide. We have examined how such variations contribute to population responses by measuring cell volumes within genetically identical populations of cells where individual members of the population are continuously growing and dividing, and we have derived a function describing the stationary distribution of cell volumes that arises from these dynamics. The model includes stochastic parameters for the variability in cell cycle times and growth rates for individual cells in a proliferating cell line. We used the model to analyze the volume distributions obtained for two different cell lines and one cell line in the absence and presence of aphidicolin, a DNA polymerase inhibitor. The derivation and application of the model allows one to relate the stationary population distribution of cell volumes to extrinsic biological noise present in growing and dividing cell cultures.

Published by Elsevier Ltd.

1. Introduction

Observations of cells in culture typically reveal a noticeable diversity of phenotypes within individual cells across the population (Bar-Even et al., 2006; Raser and O'Shea, 2005). This diversity of phenotypes occurs even when cells have identical DNA (single cell clones) and are cultured in a homogeneous environment. With imaging cytometry of individual cells, we have observed reproducible distributions in cell spread area, green fluorescent protein expression, cytoskeleton staining, and fluorescent immuno-staining (Bhadriraju et al., 2007; Langenbach et al., 2006; McDaniel et al., 2007) within monoclonal populations under highly controlled extracellular matrix conditions (Elliott et al., 2005). The diversity of cellular responses within a population of cells can also be observed in flow cytometry experiments that measure immunofluorescent-staining, expression of a fluorescent protein or cell volume. For example, flow cytometers that utilize the Coulter principle (Shapiro, 2003), which is based on an impedance change as an individual cell passes through an orifice, allow the distribution of cell volumes in a population to be measured. As with data collected by imaging cytometry, the distribution of cell volumes of continuously cultured mammalian cells appears to be stationary in that the shape of the distribution is highly reproducible over many population doublings and can be recovered after perturbation (Anderson and Petersen, 1967;

Conlon and Raff, 2003). This suggests that these distributions are a characteristic of the cell population. One likely source of cell-to-cell variability within a population comes from stochastic fluctuations within the intracellular signaling pathways through which cells respond to environmental conditions (Elowitz et al., 2002; McAdams and Arkin, 1997; Mettetal et al., 2006; Pedraza and van Oudenaarden, 2005; Volfson et al., 2006). These fluctuations can be global in nature (extrinsic) or pathway specific (intrinsic) (Ramanathan and Swain, 2005; Raser and O'Shea, 2005).

In this report, we describe how the stationary distribution of cell volumes within a population could arise due to variations in the rates of cell growth and cell division both of which are functions of variability in gene expression. We explicitly consider the role of random fluctuations in rates of cell growth and division. The model proposed here describes an asynchronous population of continuously growing and dividing cells in terms of four parameters: a mean cell cycle time, the variance in cell cycle time, a mean growth rate, and the variance in growth rates. The model is expressed as an analytic function and we demonstrate its use to evaluate cell volume distribution data to estimate these four parameters. Each of these parameters is a measurable quantity, potentially allowing validation of the model. This model provides a tool for evaluating cell cultures and for determining changes in growth or division rates within the culture that may arise due to changes in culture conditions (i.e. drug treatments or infection) or aging of the culture after many passages. The stochastic components of the model allow two different cell cultures to be compared on the basis of the relative noise in the growth and division processes in each of the cultures.

---

2. Materials and methods

2.1. Application of the cell volume distribution model

The cell culture and cell volume distribution measurement protocols are described in the Supporting information. Cell volume vs. frequency data obtained from the electronic sizing instrument was fit to the cell volume distribution model (Eq. (1) below) using non-linear least squares analysis (MathCad, Needham, MA). The fitting routines are also available in an open-source environment, 'cellVolumeDist' package (R Development Core Team, 2008). In the analysis, the doubling time was calculated from

$$t_d = \frac{\log(2) \cdot T}{\log\left(\frac{N_f}{N_o}\right)} \tag{1}$$

The doubling time, t_d, is determined from the number of cells seeded (N_o) and the number of cells (N_f) after time, T. The cell doubling time, t_d, and average cell cycle time, t, were assumed to be equivalent, though this assumption is not strictly true (Painter and Marr, 1967) (Supporting information). Four volume distribution measurements were curve fit for each of the NIH 3T3 and A10 vSMC cultures. In Table 1, the parameter value for t and its 95% confidence interval was determined from cell counts over four consecutive passages. The parameter value for σ_t was $0.3 \times t$, which is an estimate based on reported live cell microscopy measurements (Shen et al., 2006). The parameter values for r and σ_r and the 95% confidence intervals for r and σ_r were determined from the non-linear least squares curve fitting analyses. Particles smaller than 470 μm^3 were considered non-cellular and discarded from the curve fitting analysis. The integral in Eq. (8) was calculated in the interval from 0 to $6 \times t$. Increasing the interval over which the integral was calculated did not affect the fitted parameters. The coefficient of variation in the growth rate was determined as σ_r/r and the 95% confidence interval for this quotient was determined by propagating the errors in r and σ_r.

3. Results

3.1. Some characteristics of cell volume distributions

Our assumptions for the model are based, in part, on the following experimental observations. First, cells in culture divide into two daughter cells at the end of the cell cycle and thus exponentially increase in number with time. Secondly, the distribution of cell volumes in a continuously cultured population remains invariant when measured over long periods of time. Fig. 1 is a plot of cell volumes measured using a commercial cell sizing instrument that measures the volume of individual cells (Shapiro, 2003). Data for two different continuously cultured mammalian cell lines, NIH 3T3 mouse fibroblasts and A10 rat vascular smooth muscle cells (vSMCs), are depicted in this figure. Seven volume distributions measured at consecutive passages are shown for each cell type. It is apparent that even though the two cell lines were subjected to the same culture conditions (see Methods), they exhibit distinct distributions with respect to both the shape and position of the distributions on the volume axis. This suggests that genetic or gene expression variations between the cell types are likely determinants of the features of the distribution. In fact, the cell volume distribution appears to be characteristic of the cell line; cryopreserved cells can be thawed and cultured, and within a few passages, demonstrate an identical distribution to that shown in Fig. 1.

In the inset of Fig. 1 is a schematic of the growth and division processes that might give rise to the measured distribution.

Variations in growth rate and cell cycle times will occur within the population due to stochastic fluctuations in the coupled biochemical reactions that regulate cell growth and division. These variations will contribute to the width of the measured volume distribution. The position and the shape of the distribution will also likely be influenced by environmental factors such as availability of nutrients and compounds that influence cellular growth and division.

3.2. Model description

The model we present describes the distributions of cell volumes such as those shown in Fig. 1 in terms of four parameters: the mean cell cycle time, the variance in cell cycle times, the mean growth rate over the cell cycle, and the variance in growth rates within the population. The model assumes that an individual cell increases in volume at a constant rate throughout the cell cycle, and that at division a cell divides into two equally sized daughter cells. While these assumptions are simplistic, they are close approximations to data that has been measured previously for growing mammalian cells (Conlon and Raff, 2003; Dunn and Zicha, 1995; Popescu et al., 2008) and facilitate the calculations. The volume of an individual cell when it has finished growing and is ready to divide is a function of that cell's volume at 'birth' plus the increase in volume that occurs during its growth. Growth occurs between the time a daughter cell arises following division (its 'birth') and the time that it divides; that intervening time is its cell cycle time.

We assume that each cell in the population has a cell cycle time that comes from a normal distribution of cell cycle times with a mean for that population (t) and a standard deviation (σ_t). Each cell also has a growth rate that comes from a normal distribution of growth rates with a mean (r), and a standard deviation (σ_r). We assume normal distributions for cell cycle times and growth rates based on empirical observations (Miyamoto et al., 1973) and because these assumption allows for a model that is analytically tractable.
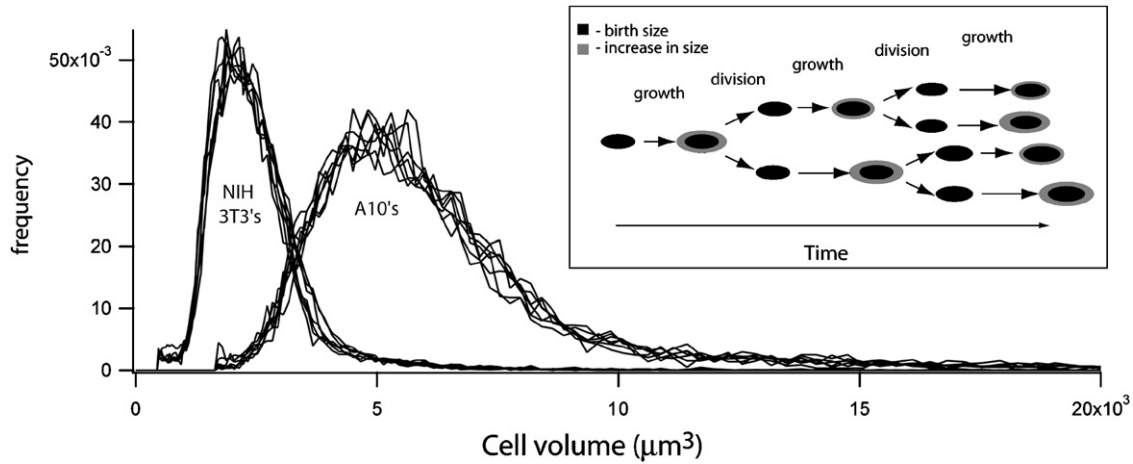
To describe the model, we use the common nomenclature for describing microbial population dynamics (Painter and Marr, 1968). The terms $\psi(V)$, $\phi(V)$, and $\lambda(V)$ are distributions that describe newly divided cells, cells ready to divide, and the entire cell population, respectively. Below, we derive the simple case where the distribution of volumes is only dependent on the average cell growth rate and the variation in cell cycle times to facilitate the description of the model construction. The derivation for the more complete model which also includes variability in growth rates is presented in the Supporting information.

The derivation begins by stating the often used relationship between the volume distributions of newly divided cells ($\psi(V)$) and cells ready to divide ($\phi(V)$), which comes from the realization that a population of newly divided cells has one-half the mean and standard deviation of a population of cells immediately prior to division (Painter and Marr, 1968).

$$\psi\left(\frac{V}{2}\right) = 2\phi(V) \tag{2}$$

Eq. (2) assumes a conservation of volume at division and that cells divide into precisely two daughter cells of equal volume. The next expression describes the growth of cells within the population where all cells increase in volume with the same growth rate, r:

$$f_{growth}(V) = \frac{1}{r \cdot \sigma_t \sqrt{2\pi}} \exp\left[\frac{-(V - r \cdot t)^2}{2(r \cdot \sigma_t)^2}\right] \tag{3}$$

Fig. 1. Cell volume distributions plotted from Coulter size measurements made over seven consecutive passages of continuously cultured NIH 3T3 cells and A10 smooth muscle cells. The mean and standard deviations for the NIH 3T3 volume distribution and the A10 smooth muscle cell distribution are $\mu = 2300\,\mu m^3$ and $\sigma = 650\,\mu m^3$ and $\mu = 5800\,\mu m^3$ and $\sigma = 1800\,\mu m^3$, respectively. INSET: schematic that describes the growth and division process that gives rise to the distribution of cell volumes.

In Eq. (3), $f_{growth}(V)$ is a Gaussian probability density function and physically represents the distribution of volumes that newly divided cells will increase by before they divide. It takes the form of a diffusion process in cell volume space plus a constant drift term (Gardiner, 2004). For cultures of continuously growing and dividing cells, the increase in volume of any individual cell due to growth during that cell's growth cycle is given by $r \times t$. Because cell cycle time, t, has a Gaussian distribution with a standard deviation, σ_t, $f_{growth}(V)$ is also a Gaussian distribution with mean, $r \times t$, and standard deviation, $r \times \sigma_t$. The following integral equation then describes how the population of newly divided cells, $\psi(V)$, in the population will increase in volume through growth and populate a distribution of cell volumes at division, $\phi(V)$.

$$\phi(V) = \int_{-\infty}^{\infty} \psi(V_\alpha) f_{growth}(V - V_\alpha)\, dV_\alpha \tag{4}$$

Eq. (4) is a convolution integral that assumes the increase in volume of a cell as it grows prior to dividing is independent from or uncorrelated with its 'birth' volume. The term V_α is introduced to compute the convolution integral over all volumes. By substituting Eqs. (2) and (3) in Eq. (4), the distribution of cell volumes in a population of newly divided cells can be expressed in terms of r, t, and σ_t (the details of the derivation are presented in the Supporting information) as shown below:

$$\psi(V) = \frac{1}{\sqrt{\frac{1}{3}(r \cdot \sigma_t)^2} \cdot \sqrt{2\pi}} e^{(-(V - rt)^2)/2(1/3(r \cdot \sigma_t)^2)} \tag{5}$$

The expression in Eq. (5) describes the probability of a newly divided cell having a volume, V, when all of the cells in the population increase in volume with a single growth rate, r. Eq. (5) can also be used to describe the distribution of cell volumes in a population of cells of a certain age, τ, by replacing t with $t+\tau$, where τ is the time after cell division. With the generalization to cells of all ages, $\tau = 0$ to $\tau = \infty$, it is now possible to describe the distribution for all cells within the asynchronous population, not just newly divided cells.

The probability that a newly divided cell will not divide in time τ, is then given by

$$\Omega(|\tau - t|) = \frac{1}{2} erfc\left(\frac{|\tau - t|}{\sigma_t \cdot \sqrt{2}}\right) \tag{6}$$

As cells in culture continue to grow they are more likely to divide. At division, the dividing cell is removed from the

population and two new daughter cells are generated. Since we assume that cells in the population exhibit a normal distribution of cell cycle times, the right hand side of Eq. (6) has the form of a complementary error function centered at the average cell cycle time, t. Using Eqs. (5) and (6) allows us to describe the entire distribution of cell volumes $\lambda(V)$ as a function of r, t and σ_t as shown:
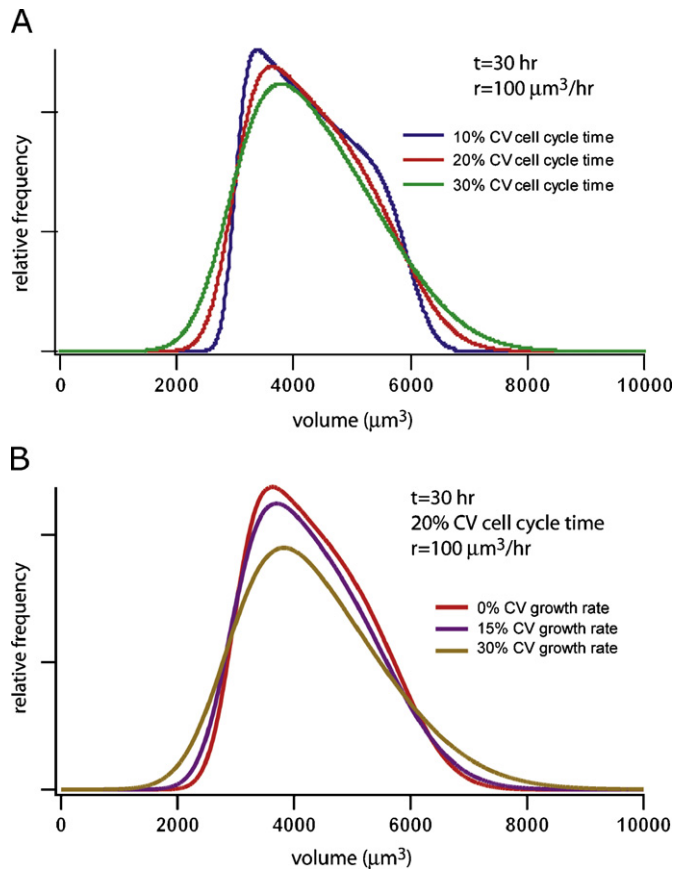
$$\lambda(V) = A \int_0^{\infty} 2^{-\tau/t} \left(\frac{1}{\sqrt{\frac{1}{3}(r \cdot \sigma_t)^2} \cdot \sqrt{2\pi}} e^{(-(V - r(t+\tau))^2)/2(1/3(r \cdot \sigma_t)^2)} \right) \times (\Omega(|\tau - t|))\, d\tau \tag{7}$$

In Eq. (7), the term A before the integral is a multiplicative constant used to normalize the area under the distribution for computing probabilities and curve fitting, and the factor $2^{-\tau/t}$ accounts for the process whereby one larger cell generates two smaller cells through division (Kubitschek, 1969). Kubitschek (1969) constructed a similar function representing the entire cell population, $\lambda(V)$, by integrating over functions for the 'birth' volume distribution and the probability that a newly divided cell will not divide in time τ. Our function is distinct compared to the function derived by Kubitschek as it relates $\lambda(V)$ to the cell cycle times and growth rates of cells in the population. With this function, the effect of variability in either cell cycle time or growth rates on the volume distribution of an asynchronous cell population can be examined. Hannsgen et al. derived several functions for the 'birth' volume distribution, $\psi(V)$, in terms of growth rates and division times (Hannsgen et al., 1985), but their approach did not yield expressions that were amenable to the analyses of the entire cell population, $\lambda(V)$.

Eq. (8) shows the more complete function for $\lambda(V)$ with the additional term, σ_r, which describes the variability of growth rates across the population of cells (see Supporting information for derivation).

$$\lambda(V) = A \int_0^{\infty} 2^{-\tau/t} \left(\frac{1}{\sqrt{\frac{1}{3}(r \cdot \sigma_t)^2 + \frac{1}{3}(t \cdot \sigma_r)^2 + (\tau \cdot \sigma_r)^2} \cdot \sqrt{2\pi}} \right.$$
$$\left. \times e^{(-(V - r(t+\tau))^2)/(2(1/3(r \cdot \sigma_t)^2 + 1/3(t \cdot \sigma_r)^2 + (\tau \cdot \sigma_r)^2))} \right) (\Omega(|\tau - t|))\, d\tau \tag{8}$$

The effect of the variations in cell cycle time and individual cell growth rates (σ_t and σ_r) on the shape of the distribution predicted by this function is shown in Fig. 2A and B, respectively. Both sets

Fig. 2. Predicted volume distributions for different levels of variance in the cell cycle times and growth rates. (A) Eq. (7) is plotted for $t = 30$ h, $r = 100 \,\mu m^3/h$ using three different values for $\sigma_t = 3$ (blue), 6 (red), and 9 (green). The coefficient of variation (CV) for each of these cases is 10%, 20%, and 30%, respectively. (B) Eq. (8) is plotted for $t = 30$ h, $r = 100 \,\mu m^3/h$, $\sigma_t = 6$ (CV cell cycle time = 20%) using three different values for $\sigma_r = 0$ (red), 15 (purple), and 30 (brown). The CV for the growth rate in each of these cases is 0%, 15%, and 30%, respectively. The CV is the standard deviation divided by the mean for the distribution. (For interpretation of the references to colour in this figure legend, the reader is referred to the web version of this article.)

Table 1
Parameter values estimated by fitting Eq. (8) to cell volume distribution data..

Cell type[a]	t[b] (h)	σ_t[c] (h)	r[d] ($\mu m^3/h$)	σ_r[d] ($\mu m^3/h$)	(σ_r/r)[e]
NIH 3T3	19.5±0.7	5.9	87±4	29±6	0.34±0.07
A10	29±3	8.7	140±20	52±7	0.37±0.07
A10 (50 nM)	36±3	10.8	139±15	57±6	0.41±0.06
A10 (100 nM)	50±8	15	115±23	51±10	0.43±0.12

[a] A10 vSMCs were continuously cultured in the absence or in the presence of 50, and 100 nM aphidicolin, as indicated.
[b] Cell cycle times (mean±95% confidence interval) estimated from the seeding density and cell counts at each of the four passages (see Methods for details).
[c] Cell cycle time variability estimates were assumed to be 0.3 of the mean cell cycle time (Shen et al., 2006).
[d] Estimates for r and σ_r were made by fitting Eq. (8) to each of the four volume distributions to calculate the mean±95% confidence interval.
[e] The estimate for the coefficient of variation in growth rate (σ_r/r) was made using the corresponding estimates for r and σ_r, then propagating the error in the measurement to calculate the mean±95% confidence interval.

of curves compare well with cell volume distributions obtained by simulating a population of cells growing and dividing with identical parameters (Supporting information). As indicated in Fig. 2A and shown explicitly in the Supporting information, the distribution has a finite width even as the 'noise' terms become small. In the limiting case where σ_t and σ_r approach 0, the coefficient of variation of the distribution is ≈ 0.52. This shows that even when the growth rates and division times are identical for all cells, the distribution has significant width caused exclusively by the asynchronous, cycling population. Increasing the noise levels in either cell cycle time or growth rate (σ_t or σ_r) increases the tail region to the left and to the right of the average. The distributions in Fig. 2 have longer tails on the right, which is also true for the measured cell volume distributions in Fig. 1.

3.3. Application of the cell volume distribution model

To test the model and demonstrate its application, we measured cell volume distribution data for NIH3T3 cells under standard culture conditions, and A10 vSMCs under standard culture conditions and conditions under which cell growth and/or division time was perturbed with drug treatment. When the DNA polymerase inhibitor aphidicolin was added to A10 vSMC cultures
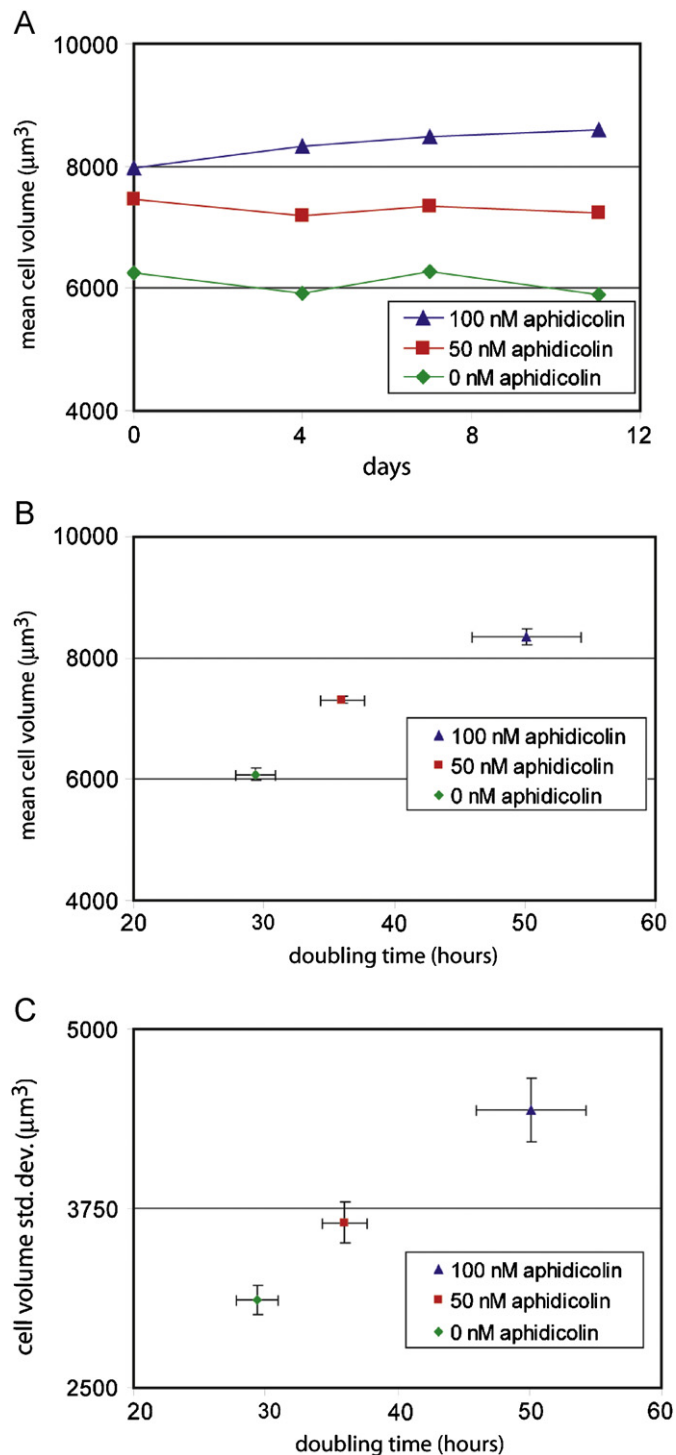
at 50 and 100 nM concentrations, the cells continued to proliferate, but exhibited longer cell cycle times that we attribute to an increase in the length of S-phase. For example, the mean doubling time of the A10 vSMCs increases from 29 to 36 h and 56 h for 50 and 100 nM aphidicolin treatments, respectively (see Table 1).

The effect of the aphidicolin treatment on the A10 vSMCs is shown in Fig. 3. After several passages under the aphidicolin treatment, the mean cell volume of the A10 vSMC increased to new values that remained stable for several additional passages (Fig. 3A). This stability suggests that the population distributions have achieved a new stationary state. Fig. 3B shows the mean cell volume plotted against the mean doubling time and indicates that the increasing doubling time with aphidicolin concentration corresponds to an increase in the mean cell volume. The standard deviation of the cell volume distributions vs. mean doubling time is plotted in Fig. 3C. This figure shows that the width of the distribution of cell volumes increases as the doubling time of the cell population increases. These results are consistent with previous observations that aphidicolin treatment can significantly increase the cell cycle time without out apparently influencing the growth rate of individual cells (Conlon and Raff, 2003).

Fig. 4 shows the measured distributions of cell volumes for NIH 3T3 cells and for A10 vSMCs in the absence or presence of aphidicolin, and the best fit distributions generated from Eq. (8) using the measured mean doubling times and assuming a 30% coefficient of variation in cell cycle times for each of the cultures (Shen et al., 2006). These plots indicate the fitted distributions show good correspondence with the measured distributions. Values for the mean growth rate of cell populations and the standard deviation in growth rate obtained from non-linear least squares fitting of the measured distribution data to Eq. (8) are shown in Table 1. Comparing the results for untreated A10 vSMCs with the results for untreated NIH 3T3 cells indicate that the growth rate (i.e., the rate of increase in cell volume), r, of A10 vSMCs is significantly higher than that for the NIH 3T3 cells ($140 \,\mu m^3/h \pm 20 \,\mu m^3/h$ for the A10 vSMCs vs. $87 \,\mu m^3/h \pm 4 \,\mu m^3/h$ for the NIH 3T3 cells). While the variability in growth rate, σ_r, is also greater for the A10 vSMCs compared to the NIH 3T3 cell line ($52 \,\mu m^3/h \pm 7 \,\mu m^3/h$ for the A10 vSMCs vs. $30 \,\mu m^3/h \pm 6 \,\mu m^3/h$ for the NIH 3T3 cells), the coefficients of variation (σ_r/r) for the growth rate variability are similar (0.34 ± 0.07 for the A10 vSMCs vs. 0.37 ± 0.07 for the NIH 3T3 cells).
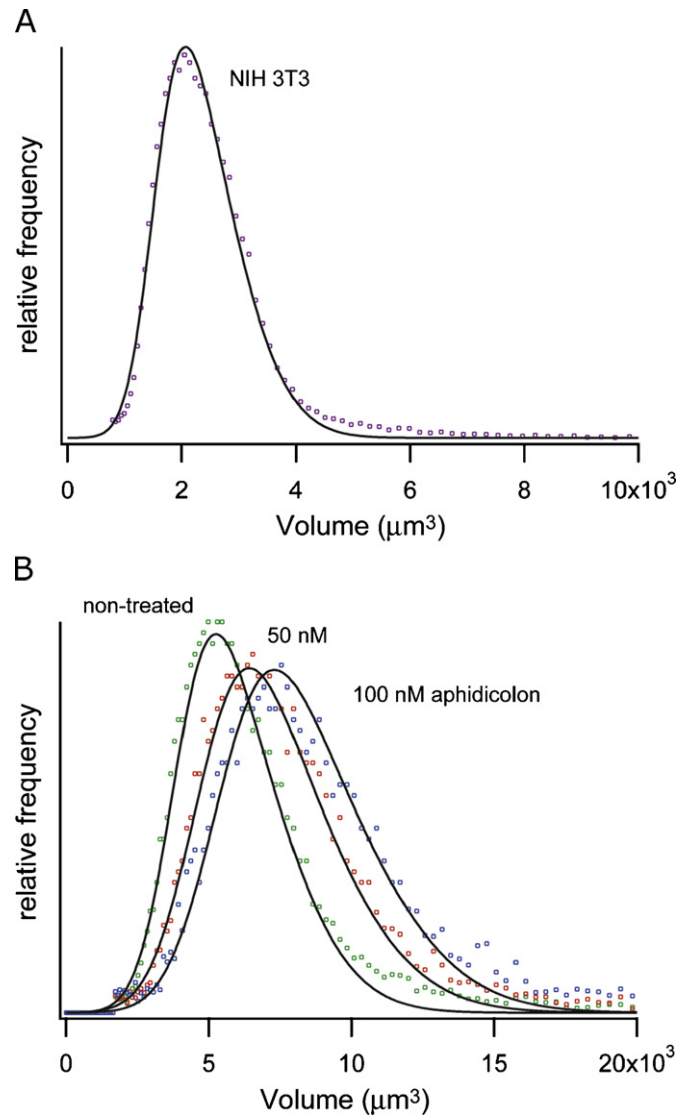
When the untreated A10 vSMCs are compared with A10 vSMCs treated with aphidicolin, the results in Table 1 indicate that the untreated cells and the cells treated with 50 nM aphidicolin

Fig. 3. Summary statistics for cell volume distributions measured from A10 vSMCs cultured in the presence of aphidicolin and 10% FBS. (A) The mean cell volumes are plotted for cultures grown in 0, 50, and 100 nM aphidicolin. The cell volumes were measured four times over a period of 11 days. (B) Volume data from (A) plotted against the doubling times ($n = 4$) (Methods) for each of the three cultures. (C) Standard deviations ($n = 4$) were calculated from the cell volume distribution data collected for (A) and plotted against the doubling times for each of the three cultures.

Fig. 4. Solid black lines represent best fits to the measured cell volume distributions with Eq. (8) using the parameter values shown in Table 1. (A) The NIH 3T3 volume distribution (purple circles) is the average of the distributions measured for a population of cells at seven different passage times (same data as in Fig. 1). (B) The A10 volume distributions (red, green, and blue circles, where the aphidicolin concentration is indicated) are the average of distributions measured for a population of cells at four different passage times (same data as in Fig. 3). (For interpretation of the references to colour in this figure legend, the reader is referred to the web version of this article.)

have similar growth rates ($140\,\mu m^3/h \pm 20\,\mu m^3/h$ vs. $139\,\mu m^3/h \pm 15\,\mu m^3/h$), and that the growth rate is reduced when cells are treated with 100 nM aphidicolin ($115\,\mu m^3/h \pm 23\,\mu m^3/h$). Despite the reduction of the growth rate, the coefficients of variation (σ_r/r) for the growth rate variability for the A10 vSMCs with no aphidicolin, 50 nM aphidicolin, and 100 nM aphidicolin are similar (0.37 ± 0.07, 0.41 ± 0.06, and 0.44 ± 0.12, respectively). This suggests that the biochemical mechanisms responsible for the variations in growth rate appear to scale with the mean growth rate from the cell.

4. Discussion

Many population models have been developed for the analysis of cell size distributions (18,20) and several attempts have been made to deduce the mean growth behavior of cells as a function of their volume (Bell and Anderson, 1967; Collins and Richmond, 1962; Koch and Higgins, 1982) and to understand whether cells increase in volume exponentially or at a constant rate (Kubitschek, 1969). Observations made from cells growing in

culture resulted in the 'transition probability model' (Smith and Martin, 1973), where cell cycle progression depends on the completion of a probabilistic A-phase (similar to a G1 cell cycle phase) which cells can exit with a constant probability per unit time before entering a B-phase (similar to a combined S, G2 and M phase) for a deterministic length of time that ends with cell division. Hannsgen et al. reported a detailed mathematical description for several aspects of the cell volume distributions that would result when cell cycle times follow the 'transition probability' model (Hannsgen et al., 1985; Hannsgen and Tyson, 1985).

Although our model borrows many of the conventions and assumptions used in these earlier models, it differs from these models with the use of four cell-based parameters, mean growth rate, mean cell cycle time, variance in growth rate and variance in cell cycle time to describe the stationary distributions of cell volumes that arise from continuously growing cell cultures. These parameters are directly related to the physical processes that give rise to the distribution of cell volumes. While other distribution functions such as a log-normal have been used to generate parameters that are characteristic of cell cultures (Kaneko and Furusawa, 2008), the model presented here has the advantage of being based on parameters with inherent physical meaning.

One of the parameters in the model that could be useful for characterizing cellular responses is the average growth rate of single cells in the culture. Single cell growth rates are difficult to measure in adherent mammalian cells and therefore are infrequently used to characterize cell populations. The analysis above provides comparative data on two cell lines and indicates that on average A10 vSMCs increase in volume approximately 1.7 fold faster than NIH 3T3 cells. Many processes are likely to control the rate at which cells increase in volume including glucose uptake, protein biosynthesis, and other metabolic functions. While the molecular origin of the growth rate differences between the A10 vSMCs and the NIH 3T3s is unclear and is probably quite complex, this method provides a quantitative method for comparing the rates of cell growth between different cell lines.

The model can also be used to characterize changes in growth rate or doubling times of a cell line in response to changes in culture conditions. The addition of low doses of aphidicolin to A10 cells apparently increases both the doubling time and the mean cell volume (Fig. 3B). Applying the model in Eq. (8) to the volume distributions indicates the growth rates calculated for the non-treated A10 vSMCs and the cultures grown in the presence of 50 nM aphidicolin were comparable, even as cell division times and cell volumes increased (see Table 1 and Fig. 3A). Interestingly, the volume growth rate of the A10 vSMCs cells treated with 100 nM aphidicolin is apparently reduced to approximately 80% of the growth rate for the non-treated cells and those treated with 50 nM aphidicolin (see Table 1). As with the comparison between the A10 vSMCs and the NIH 3T3 cell lines, the molecular origin of the growth rate differences is unknown. It is likely that one or several of the pathways known to regulate cell growth and division such as PI3K, mTOR, Akt, and Myc (Proud, 2007) are affected when A10 vSMCs are cultured in 100 nM aphidicolin. These results demonstrate that changes in cell volume distributions can likely provide indication of, and insight into changes in the growth and division process of a cell line due to age, phenotype and perturbations to the culture conditions.

The model presented here also allows estimation of the noise in cell cycle times and in cell growth within a clonal population. The noise terms, σ_t and σ_r, appear to influence the shape of the distribution of cell volumes as illustrated in Fig. 2. Therefore, the model can be used to evaluate the level of noise present in the cellular processes that give rise to the cell volume distribution. Biological noise is an inherent property of cellular systems

because of the coupled biochemical reactions and feedback signals that organize cellular processes including progression through the cell cycle and the synthesis of cellular material. In the analysis shown in Fig. 4 and Table 1, a 30% coefficient of variation in cell cycle time is used as an estimate based on previously reported observations (Shen et al., 2006). While it is likely that the actual variations in cell cycle times are different between the cultures used in this study, this assumption allows the comparison of the relative noise in the growth rates (σ_r/r). The values for σ_r/r (Table 1) are similar for the NIH 3T3 cells, the non-treated A10 vSMCs, the 50 nM aphidicolin treated A10 vSMCs, and the 100 nM aphidicolin treated A10 vSMCs. This suggests that under all conditions examined, the cultures have similar levels of relative noise in the growth and division process, which is interesting considering the cell cycle times and growth rates vary significantly between all of the cultures. Furthermore, the noise parameters that are calculated from fitting the model to cell volume distribution data could be compared with or used to guide the noise parameters used in more detailed cellular systems biology models, such as those used for cell signaling pathways where stochastic terms are included.

There are several caveats related to interpreting the noise terms in Eq. (8). The first is that the cell cycle time and growth rate distributions are represented as simple Gaussian distributions in the model. Although more sophisticated models that explicitly account for specific molecular components and interactions could be integrated in the future, this assumption of Gaussian distributions allows derivation of an analytical solution that can be applied to routinely collected cell volume distribution measurements. Secondly, there is no term that accounts for the asymmetric division of cells. Any asymmetry in the division process will lead to an increase in the width of the distribution size of newly divided cells. This increased 'noise' in the system would be expected to increase the predicted values in the σ_t and σ_r terms. A third caveat is that the model cannot be used to extract all four parameters simultaneously from a single volume distribution measurement. This is because cell cycle time variability and growth rate variability have similar effects on the overall shape of the distribution (Fig. 2). However, each of the noise terms can be measured independently. Cell cycle time variability can be measured by timelapse microscopy of cells in culture (Killander and Zetterberg, 1965; Shen et al., 2006) and, though studied less frequently, growth rate variability can be measured using interference microscopy techniques (Dunn and Zicha, 1995; Zicha et al., 1999). Therefore, if either of the parameters is measured independently, then the other noise parameter can be estimated using the model.

In this study, we developed a model based on a constant rate of volume increase throughout the cell cycle, though the rate can vary between cells in the population, and applied the model to the analysis of cell volume distributions. We chose to analyze volume distributions because of the ease with which the data can be collected with conventional cell sizing instruments and the potential for these data to be used as a practical approach for characterizing cells in culture. It is important to note that this model can also be applied to cellular fluorescence distribution data measured by flow cytometry or automated microscopy. Live cell imaging experiments have shown that at least some proteins appear to be synthesized at a constant rate over the cell cycle (Sigal et al., 2006), and in those cases the model described here could be used to calculate parameters directly linked to the production rate of protein expression from measured steady-state distribution data. Furthermore, measured distributions that cannot be well fit to the model described here likely indicate that the production rate of the protein of interest is not constant throughout the cell cycle.

5. Conclusions

The growth and division of cells in culture is inherently 'noisy' because of the stochastic nature of biochemical reactions that govern cell cycle progression and growth. We derived an expression that relates the stationary cell volume distribution exhibited by continuously cultured mammalian cells to the cell cycle times and growth rates of individual cells in the culture. An expression is derived that relates cell volume distributions to the mean cell cycle time, standard deviation of cell cycle times, growth rates, and standard deviation of growth rates. By fitting the model to measured cell volume distributions, parameters can be calculated that are related to the physical processes that give rise to the distribution. The analysis of cell volume distribution data can indicate changes in the growth and division behavior of cultures, and the model described here provides a conceptual framework for the interpretation of these measured distributions. Such information could be used to quality control culture systems, to complement molecular biology techniques for understanding signaling pathways that effect growth and division, and to quantify the noise in cell cycling and growth. The variables generated with this model may also be useful as a starting point for more complex models of noise associated with specific pathways which also are influenced by cell cycle and growth.

Appendix A. Supplementary material

Supplementary data associated with this article can be found in the online version at doi:10.1016/j.jtbi.2008.10.031.

References

Anderson, E.C., Petersen, D.F., 1967. Cell growth and division. II. Experimental studies of cell volume distributions in mammalian suspension cultures. Biophys. J. 7, 353.

Bar-Even, A., Paulsson, J., Maheshri, N., Carmi, M., O'Shea, E., Pilpel, Y., Barkai, N., 2006. Noise in protein expression scales with natural protein abundance. Nat. Genet. 38, 636.

Bell, G.I., Anderson, E.C., 1967. Cell growth and division. I. A mathematical model with applications to cell volume distributions in mammalian suspension cultures. Biophys. J. 7, 329.

Bhadriraju, K., Elliott, J.T., Nguyen, M., Plant, A.L., 2007. Quantifying myosin light chain phosphorylation in single adherent cells with automated fluorescence microscopy. BMC Cell Biol. 8, 43.

Collins, J.F., Richmond, M.H., 1962. Rate of growth of Bacillus cereus between divisions. J. Gen. Microbiol. 28, 15.

Conlon, I., Raff, M., 2003. Differences in the way a mammalian cell and yeast cells coordinate cell growth and cell-cycle progression. J. Biol. 2, 7.

Dunn, G.A., Zicha, D., 1995. Dynamics of fibroblast spreading. J. Cell Sci. 108 (3), 1239.

Elliott, J.T., Woodward, J.T., Langenbach, K.J., Tona, A., Jones, P.L., Plant, A.L., 2005. Vascular smooth muscle cell response on thin films of collagen. Matrix Biol. 24, 489.

Elowitz, M.B., Levine, A.J., Siggia, E.D., Swain, P.S., 2002. Stochastic Gene Expression in a Single Cell. Science 297, 1183.

Gardiner, C.W., 2004. Handbook of Stochastic Methods for Physics, Chemistry, and the Natural Sciences. Springer, Berlin.

Hannsgen, K.B., Tyson, J.J., 1985. Stability of the steady-state size distribution in a model of cell growth and division. J. Math. Biol. 22, 293.

Hannsgen, K.B., Tyson, J.J., Watson, L.T., 1985. Steady-state size distributions in probabilistic models of the cell-division cycle. SIAM J. Appl. Math. 45, 523.

Kaneko, K., Furusawa, C., 2008. Consistency principle in biological dynamical systems. Theory Biosci. 127, 195.

Killander, D., Zetterberg, A., 1965. Quantitative cytochemical studies on the interphase growth. I. Determination of DNA, RNA and mass content of age determined mouse fibroblasts *in vitro* and of intercellular variation in generation time. Exp. Cell Res. 38, 272.

Koch, A.L., Higgins, M.L., 1982. Cell cycle dynamics inferred from the static properties of cells in balanced growth. J. Gen. Microbiol. 128, 2877.

Kubitschek, H.E., 1969. Growth during bacterial cell cycle—analysis of cell size distribution. 9, 792.

Langenbach, K.J., Elliott, J.T., Tona, A., McDaniel, D., Plant, A.L., 2006. Thin films of type 1 collagen for cell by cell analysis of morphology and tenascin-C promoter activity. BMC Biotechnol. 6, 14.

McAdams, H.H., Arkin, A., 1997. Stochastic mechanisms in gene expression. Proc. Nat. Acad. Sci. USA 94, 814.

McDaniel, D.P., Shaw, G.A., Elliott, J.T., Bhadriraju, K., Meuse, C., Chung, K.H., Plant, A.L., 2007. The stiffness of collagen fibrils influences vascular smooth muscle cell phenotype. Biophys. J. 92, 1759.

Mettetal, J.T., Muzzey, D., Pedraza, J.M., Ozbudak, E.M., van Oudenaarden, A., 2006. Predicting stochastic gene expression dynamics in single cells. Proc. Nat. Acad. Sci. USA 103, 7304.

Miyamoto, H., Zeuthen, E., Rasmussen, L., 1973. Clonal growth of mouse cells (strain L). J. Cell Sci. 13, 879.

Painter, P.R., Marr, A.G., 1967. Inequality of mean interdivision time and doubling time. J. Gen. Microbiol. 48, 155.

Painter, P.R., Marr, A.G., 1968. Mathematics of microbial populations. Ann. Rev. Microbiol. 22, 519.

Pedraza, J.M., van Oudenaarden, A., 2005. Noise propagation in gene networks. Science 307, 1965.

Popescu, G., Park, Y., Lue, N., Best-Popescu, C., Deflores, L., Dasari, R.R., Feld, M.S., Badizadegan, K., 2008. Optical imaging of cell mass and growth dynamics. Am. J. Physiol. Cell Physiol. 295, C538.

Proud, C.G., 2007. Signaling to translation: how signal transduction pathways control the protein synthetic machinery. Biochem. J. 403, 217.

R Development Core Team, 2008. R: A language for statistical computing. R Foundation for Statistical Computing. ISBN 3-900051-07-0, URL:http://www.R-project.org.

Ramanathan, S., Swain, P.S., 2005. Tracing the sources of cellular variation. Dev. Cell 9, 576.

Raser, J.M., O'Shea, E.K., 2005. Noise in gene expression: origins, consequences, and control. Science 309, 2010.

Shapiro, H.M., 2003. Practical Flow Cytometry. Wiley-Liss, Hoboken N.J.

Shen, F., Hodgson, L., Rabinovich, A., Pertz, O., Hahn, K., Price, J.H., 2006. Functional proteometrics for cell migration. Cytometry A 69, 563.

Sigal, A., Milo, R., Cohen, A., Geva-Zatorsky, N., Klein, Y., Alaluf, I., Swerdlin, N., Perzov, N., Danon, T., Liron, Y., Raveh, T., Carpenter, A.E., Lahav, G., Alon, U., 2006. Dynamic proteomics in individual human cells uncovers widespread cell-cycle dependence of nuclear proteins. Nat. Methods 3, 525.

Smith, J.A., Martin, L., 1973. Do cells cycle? Proc. Nat. Acad. Sci. USA 70, 1263.

Volfson, D., Marciniak, J., Blake, W.J., Ostroff, N., Tsimring, L.S., Hasty, J., 2006. Origins of extrinsic variability in eukaryotic gene expression. Nature 439, 861.

Zicha, D., Genot, E., Dunn, G.A., Kramer, I.M., 1999. TGFbeta1 induces a cell-cycle-dependent increase in motility of epithelial cells. J. Cell Sci. 112 (Pt 4), 447.